Chapter 5

Development of Tumor-Specific Caffeine-Potentiated Chemotherapy Using Span 80 Nano-Vesicles DDS

Tatsuhiko Miyazaki, Hiroshi Nakata and Keiichi Kato

Additional information is available at the end of the chapter

http://dx.doi.org/10.5772/intechopen.69155

Abstract

Osteosarcoma cases with metastasis have poor prognosis in general. Recently, caffeine-potentiated chemotherapy, which is chemotherapy with caffeine dosage against malignancies, has manifested potently high efficacy as well as diverse effects. Recently, we demonstrated that nonionic vesicles prepared from Span 80 have promising physicochemical properties, which let them an attractive option besides the common liposomes. Here, we manifested the tumor-specific caffeine-potentiated chemotherapy against osteosarcoma in murine model employing a novel drug delivery system (DDS) with Span 80 nano-vesicles. C3H/HeJ mice underwent transplantation of LM8 osteosarcoma cell line and then were doped with therapeutic agents. Caffeine was employed as an enhancer in addition to ifosfamide (IFO) as the antitumor agent. in vitro, the united administration of IV + CV revealed significant induction of tumor apoptosis in the early phase. In vivo study manifested that IV + CV-administration markedly decreased the tumor volume as well as the viable tumor area than in the other groups. No marked organ damage was observed in the IV or IV + CV groups as well as fertility injury and/or malformations in their progeny. This novel DDS might have the importance for clinical application in primary tumors as well as the metastatic osteosarcoma.

Keywords: DDS, Span 80 nano-vesicles, caffeine-potentiated chemotherapy, mouse model

1. Introduction

At present, osteosarcoma cases with metastasis, especially in lungs, have poor prognosis [1, 2]. In recent years, caffeine-potentiated chemotherapy, which is chemotherapy with caffeine

dosage against malignancies, has manifested potently high efficacy [3, 4]. Nevertheless, this method may induce adverse effects that patients suffer, which include most commonly tachycardia, nausea, psychiatric symptoms, as well as lethal arrhythmia with individual diversity [5]. On the other hand, there have been numerous developments in novel drug delivery systems (DDSs) for drug carriers for the treatment of various diseases that enabled target-specific drug delivery resulting in the prevention of side effects [6–8].

Recently, we demonstrated that nonionic vesicles prepared from Span 80 have promising physicochemical properties, such as high membrane fluidity associated with low-phase transition temperature, which make them an attractive possible alternative to the commonly used liposomes. Lipid vesicles have been extensively studied. Since the discovery of mechanism for liposome by Bangham et al. that aqueous phase of phosphatidylcholines includes self-closed phospholipid bilayers, which can capture and obtain water-soluble molecules [9], lipid vesicles have been actively investigated. Following early reports on vesicle formation from completely synthetic amphiphiles [10], vesicles have been prepared from a large number of different surfactants [11, 12]. Many vesicle systems have been characterized to some extent and applied in various research areas, ranging from pharmaceuticals [12–15], food technology [12, 16, 17], and analytical applications to origin-of-life [18, 19] and artificial cell studies [20]. Vesicles based on nonionic surfactants (so-called "niosomes") [12, 21] were first used in the cosmetic industry [10, 21, 22] as alternatives to phospholipid-based vesicles (liposomes). One of the many surfactants used for niosome preparations is Span 80, a cheap, molecularly heterogeneous nonionic surfactant that is also applied as food emulsifier and in oral pharmaceuticals [23, 24]. Span 80 is known as sorbitan mono-oleate generally; nevertheless, commercially available Span 80 may be a heterogeneous mixture of sorbitan mono-, di-, tri, and tetra-esters which could let high fluidity and vascular permeability [25–27].

A successful therapeutic murine model of transplanted colon cancer employs the DDS using Span 80 vesicles which have immobilized polysaccharides [28]. In this chapter, we introduce a novel DDS by using Span 80 nano-vesicles, and manifested that tumor-specific caffeine-potentiated chemotherapy for murine osteosarcoma using a novel DDS with Span 80 nano-vesicles showed significant antitumor effects, as well as limited adverse effects.

2. Span 80 nano-vesicles

2.1. Characteristics of Span 80 as a material for food and pharmaceuticals

As mentioned above, Span 80 is known as sorbitan mono-oleate; nevertheless, commercially available Span 80 might be heterogeneous mixture, rather mainly diesters, in addition to triesters and tetraesters [23, 25]. Furthermore, the polar headgroup of the different esters present in Span 80 is not sorbitol, but more likely one of the different forms of anhydrized sorbitol [29, 30], a cheap, molecularly heterogeneous nonionic surfactant that is also applied as food emulsifier and in oral pharmaceuticals [31]. The substantial molecular heterogeneity of commercial Span 80 is (i) a consequence of the conditions used for the synthesis (reaction of sorbitol with fatty acids (mainly

oleic acid) at elevated temperature) [24, 29] and (ii) based on the fact that there are no purification method following the synthesis with excellent cost-performance ratio for yielding inexpensive products and applicable to large-scale purification. Commercially available Span 80 was determined by its molecular composition. The property of it may even be better when compared to the properties of the individual purified components of commercially available Span 80.

2.2. Preparation of Span 80 nano-vesicles in different forms

In our study, we prepared several variations of Span 80 vesicles as follows: Commercially available Span 80 was processed using the two-step emulsification method (Span 80 vesicles type 1), sequentially extruded by a polycarbonate membrane (Span 80 vesicles type 2) or ultrafiltrated (Span 80 vesicles type 3). Fractionation of commercially available Span 80 by chromatography into the different ester groups (see **Figure 1**) and vesicular preparation using the defined mixture of the four kinds of different ester groups (Span 80 vesicles type 4) or preparation from the diester fraction (Span 80 vesicles type 5) were performed [25].

2.3. Evaluation of diameter and homology by a dynamic light scattering

Vesicle characterization by dynamic light scattering (DLS) and electron microscopy was performed. The different types of Span 80 vesicles prepared either in distilled water or in phosphate-buffered saline (PBS) solution were analyzed after vesicle preparation by dynamic light scattering. As expected from the different preparation methods used, the average vesicle size and size distribution depend on the vesicle type, independent of whether PBS or distilled water was used as aqueous medium. (a) The vesicle size would depend on the employed method; therefore, the prepared Span 80 vesicles should be kinetically trapped aggregates and might not have thermodynamically equilibrium structures, just like most of phosphatidylcholine vesicles. (b) The most homogeneous vesicles with the lowest polydispersity index were prepared by the extrusion method. When employing PBS as the aqueous medium, the size of Span 80 vesicle type 1 with an apparent size of 250 ± 45 nm, which was obtained by DLS, could be reduced into 105 ± 13 nm by extrusion through polycarbonate membranes with a nominal pore diameter of 100 nm. Extrusion method enabled to make more homogeneous vesicles with less polydispersity index. Span 80 vesicles type 2 manifested the appropriate diameter (c.a. 100 nm) for the drug delivery; therefore, these types of vesicles were employed for further analyses in the development of DDS.

2.4. Evaluation of diameter and physicochemical property by electron microscopy

Span 80 vesicles type 2 (100 nm) prepared in PBS was also statistically analyzed by cryo-transmission electron microscopy (cryo-TEM, **Figure 1A**), yielding a number-weighted average vesicle size of 63. This value is lower than the *z*-average value (scattering intensity weighted) determined by DLS. Next, the hydrodynamic diameter was evaluated; on the other hand, in cryo-TEM images, the projected, "true" size of a spherical vesicle was obtained. The discrepancy among these methods could be addressed that the electron dense headgroup area made vesicles more boundary. Conclusively, electron microscopy revealed the diameter and bilayer thickness of the vesicles by Cryo-TEM, as well as the presence of uniformity of the vesicles by freeze fracture

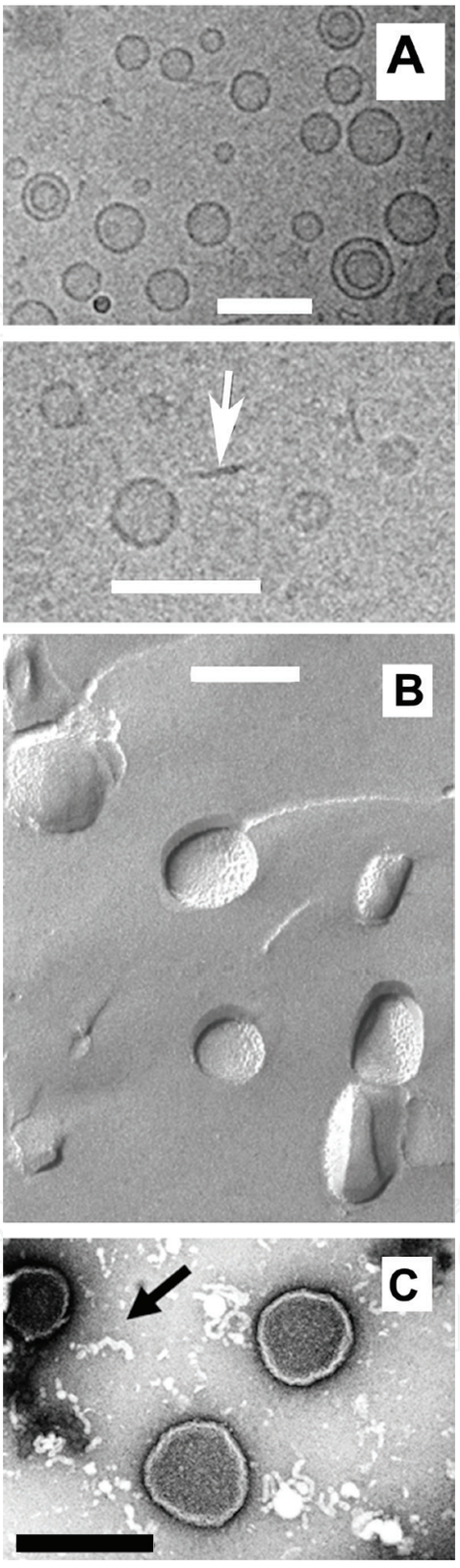

Figure 1. Electron microscopic analysis of Span 80 vesicles type 2 (100 nm), prepared in PBS. (A) Cryo-TEM micrographs showing unilamellar- and bilamellar vesicles and bilayer fragments (arrow). Length of the bar: 100 nm. Freeze fracture (B) and negative-staining (C) electron micrographs of Span 80 vesicles type 2 (100 nm), prepared in PBS solution. Length of the bar: 100 nm. The arrow in C points to one of the fragments present. [Reprinted with permission from Ref. [25]. Copyright (2008) American Chemical Society].

scanning electron microscopy (**Figure 1**). Electron micrographs revealed that Span 80 vesicle suspensions contain not only vesicles but also bilayer fragments. The clear contrast was observed among 1-palmitoyl-2-oleoyl-sn-glycero-3-phosphocholine (POPC) or dioleoylphosphatidylcholine (DOPC) vesicles which might be due to the molecular heterogeneity of Span 80 vesicles.

2.5. Temperature sensitivity of Span 80 vesicles

The temperature sensitivity of Span 80 vesicles might not link directly to the T_m value, because the observed fusion phenomenon did not develop at T_m as the temperature-sensitive vesicles based on 1,2-dipalmitoyl-sn-glycero-3-phosphocholine (DPPC) [32]. In DPPC-based vesicles, the thermos-responsive effect is the leakage of the aqueous contents when the temperature reaches T_m [33].

The Span 80 vesicles develop fusion in response to an increase in temperature. Therefore, the molecular mechanisms of thermos-response in each kind of vesicles are different. The presence of bilayer fragments in fused Span 80 vesicles at an elevated temperature is not clear at this moment. However, the nonionic headgroup in Span 80 could be dehydrated and result in vesicle-vesicle aggregation and fusion at the temperature above T_m.

2.6. Vesicle membrane fusion property

The vesicle fusion property may be advantageous for efficient drug delivery, and applications of the several types of Span 80 vesicles described and characterized in this chapter, and previous papers largely depend on the vesicle's cytotoxicity. Although previous studies of Span 80-based vesicles regarding cytotoxicity either as a drug carrier or as a gene vector were successful, further studies have been required before any conclusions with respect to pharmaceutical applications [25] can be drawn. Among the various types of Span 80 vesicles investigated, Span 80 vesicles type 2 (100 nm) might be the most attractive one (straightforward methodology with the requirement of simple equipment only).

3. Caffeine-potentiated chemotherapy using Span 80 nano-vesicles' DDS

We developed the murine osteosarcoma therapeutic model of caffeine-potentiated chemotherapy. In this model, as the therapeutic agents, ifosfamide (IFO) was employed as well as caffeine sodium benzoate (CSB) as an enhancer. As the murine osteosarcoma therapeutic model, C3H/HeJ mice underwent transplanted murine osteosarcoma cell line LM8. The detailed procedures were described in the original paper [34].

3.1. Preparation of Span 80 nano-vesicles

Span 80 nano-vesicles, which contained IFO and/or caffeine, were freshly prepared as previously described [28]. Briefly, materials for assembling nano-vesicles containing Span 80 and Tween-80 [35], cholesterol, which worked as the stabilizer of the membrane, polyethylene glycol, used as a stealth modifier against macrophages [28], and the solvents, normal hexane and normal saline, were purchased, respectively. All processes were performed under sterilized conditions.

The two-step emulsification method was employed to process and purify the nano-vesicles. Span 80 and cholesterol were dissolved in hexane by homogenization with a micro-homogenizer in a sterilized brown glass bottle. Sequentially, the first emulsion was prepared by adding IFO and/or CSB, which dissolved in normal saline into the Span 80 material followed by homogenization. As a negative control, phosphate-buffered saline was dripped alternatively. The second-stage emulsion was processed by evaporation using a rotary vacuum evaporator on a water bath at 37°C followed by homogenization with Tween-80.

The second emulsion was centrifuged using ultra-centrifugation equipment. After aspiration of the supernatant, the sediment of the Span 80 vesicles was weighed and then suspended in normal saline at a concentration of 20% w/v. By this method, IFO Span 80 vesicles (IV), CSB Span 80 vesicles (CV), and PBS-alone Span 80 vesicles (PV) were prepared. Immediately before the use *in vivo* or *in vitro*, these suspensions became extruded by a custom-made extruder with a drain disk of 100-μm thickness and a Nucleopore membrane® of 100-nm pore size to control the vesicular size. As a result, the diameter of the vesicles was evaluated by the dynamic light-scattering device and revealed 117 nm at average.

3.2. In vitro evaluation of the antitumor effects of the nano-vesicles

The murine osteosarcoma cell line, LM8, was obtained and employed as an osteosarcoma model. LM8 cells in Dulbecco's modified Eagle's medium were plated and cultured in 24-well culture dishes for a few days until the cells showed semi-confluent state. Next, antitumor agents with or without Span 80 vesicles, including PV, IV, CV, direct administration of IFO or CSB, as well as the combination of IV + CSB, IFO + CV and IV + CV were administered. Cells were incubated with the antitumor agents at 37°C for 1 or 2 h, and then the cells were harvested and evaluated for apoptosis and cell viability, respectively.

In vitro analyses revealed cultured LM8 murine osteosarcoma cells with IV + CV almost complete cell death by the trypan blue assay, on the other hand, PBS, CSB, PV, and CV manifested almost no cell death. IFO resulted in 13%, IV resulted in 28%, and IFO + CV resulted in 75% cell death (**Figure 2** and **Table 1**).

3.3. Apoptosis detection by propidium iodide (PI) method

Briefly, cells were suspended in ice-cold Hank's balanced saline solution (HBSS), followed by fixation with 70% EtOH at −20°C [36]. Fixed cells were centrifuged, then pellets were re-suspended in extraction buffer of pH 7.8 which contained Na_2HPO_4, citric acid, and 0.1% Triton X-100 at 37°C. Then, a staining solution of pH 6.8 containing PIPES, NaCl, Mg_2Cl, Triton X-100, PI, and 50 RNAse H was added to the cell suspension, and the fluorescence intensity was evaluated and analyzed in triplicate by the FACStation® and CellQuest® software.

PI analyses revealed that almost cell population (97%) underwent apoptotic cell death, which treated with IV + CV. By contrast, PBS, CSB, PV, and CV conducted cell death in very limited population, while IFO and IV let the small population into apoptosis and/or necrosis (8.8–10.2%), as well as IFO + CSB and IV + CSB induced increasing cell death to approximately a quarter to one-third of the population (**Figure 3** and **Table 2**).

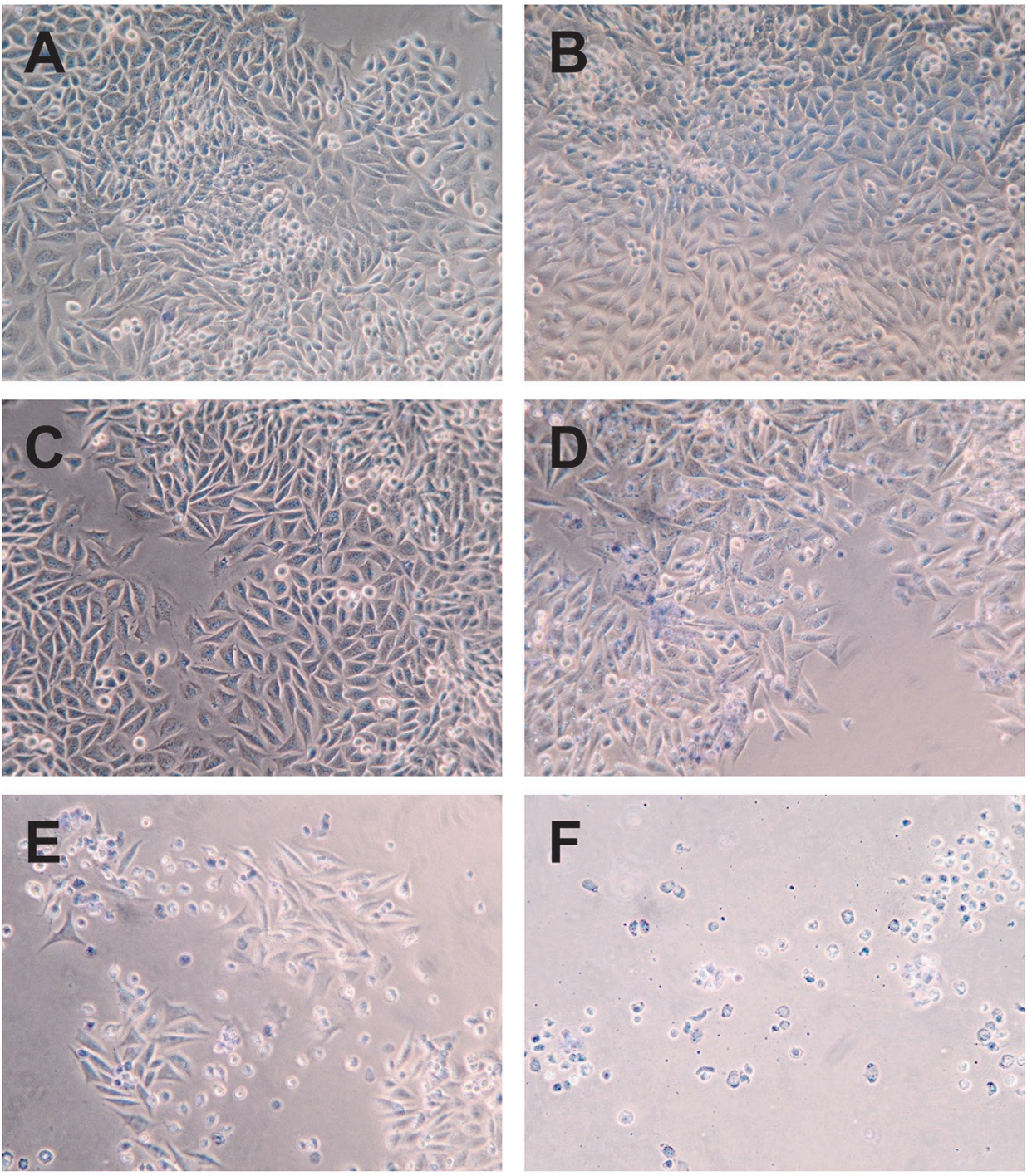

Figure 2. Representative photomicrographs of the trypan blue-stained LM8 cells after a 2-h incubation with antitumor agents: (A) PV, (B) CV, (C) IFO, (D) IV, (E) IFO + CV, and (F) IV + CV. [Reprinted with permission from Ref. [34]. Copyright (2014) Spandidos Publications].

3.4. Murine osteosarcoma therapeutic model

For the therapeutic model, C3H/HeJ mice were employed because they are H2-matched to LM8 osteosarcoma cell line since this cell line was originated from that strain of mouse [37]. LM8 cells (3.0×10^6 cells per mice) were subcutaneously transplanted into 6-week-old male

Treatment	Population of nonviable cells (%) (mean ± SD)
PBS	1.5 ± 0.9
CSB	2.1 ± 1.2
PV	3.3 ± 1.8
CV	3.1 ± 1.9
IFO	13 ± 3.4[a]
IV	28 ± 5.5[a]
IFO + CSB	25 ± 6.7[b]
IV + CSB	40 ± 9.2[c]
IFO + CV	75 ± 10.8[d]
IV + CV	98 ± 1.2[e]

[a]$P < 0.05$ versus PBS, CBS, PV, and CV.
[b]$P < 0.05$ versus PBS, CSB, PV, CV, and IFO.
[c]$P < 0.01$ versus IFO, $P < 0.05$ versus IV and IFO + CSB.
[d]$P < 0.01$ versus IV + CSB and the other groups
[e]$P < 0.05$ versus IFO + CV, $P < 0.01$ versus the other groups.

Table 1. Nonviable cell population in trypan blue analysis.

C3H/HeJ mice. After c.a. 3 weeks, when the tumor volume reached up to 500 mm^3, injection of the therapeutic agents was started. The administration protocol is schemed in **Figure 4**.

The agents were administered individually or in combinations as follows: PBS (i.v., sham administration), CV (0.1 mg/g BW), IFO (direct i.v. 0.1 mg/g BW), IV (i.v. 0.1 mg/g BW), IV + CSB, and IV + CV. Five to eight animals in each groups were analyzed in the study. The therapeutic agents were intravenously administered via tail vein on days 0, 2, and 4, followed by the harvest under anesthesia on day 7. Tumor diameter as well as the body weight of each individual was measured every day. At the time of the harvest, volumes and weights of tumors were evaluated; subsequently, the entire organs and the tumors were processed for histopathological analyses.

No significant differences were noted in body weights among each other in the groups. It was marked that the tumor volumes in the IV + CV group were reduced as compared to those of the control groups (PBS and CV), as well as a tendency toward a decrease against the PV- and IFO-direct i.v. groups on days 5–7 (**Figure 5**) could be shown.

3.5. Histopathological analyses

The histopathological analyses of the harvested tumors and entire organs were executed on the formalin-fixed, paraffin-embedded tissue section. The area of viable tumor was evaluated as the viability of the tumor tissue in hematoxylin-eosin (HE)-stained sections. Next, in order to determine the adverse effects, entire organ tissue sections stained with HE, periodic acid-Schiff (PAS), and Elastica-Goldner stains were accessed by skilled pathologists.

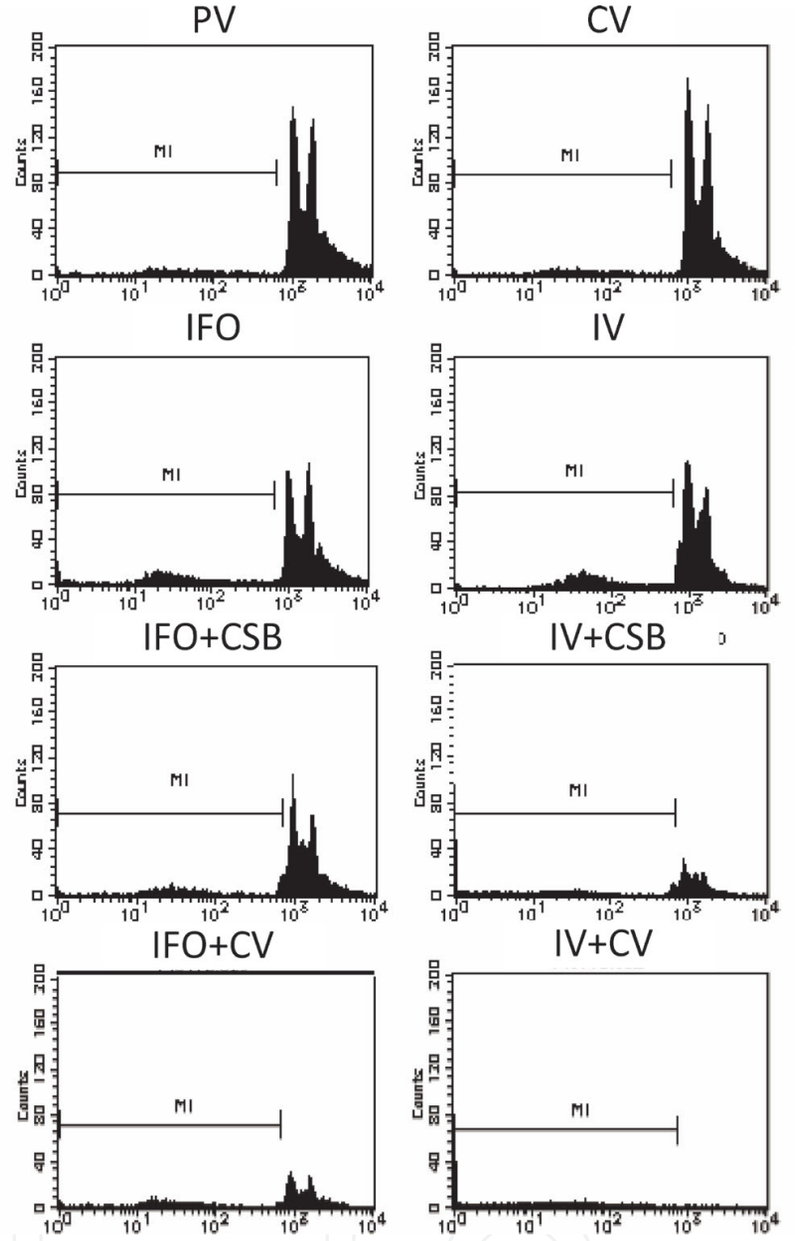

Figure 3. The PI-staining apoptosis assay using flow cytometry. Each panel shows the event count (vertical axis) at each intensity (horizontal axis). The population of apoptotic and/or necrotic cells was measured as M1 and was shown in Table 2. [Reprinted with permission from Ref. [34]. Copyright (2014) Spandidos Publications].

IFO, IV, IV + CSB, and IV + CV groups revealed significantly smaller viable tumor areas in comparison to the controls. Moreover, the IV + CV group revealed markedly reduced viable tumor areas against the IFO and IV groups (**Figures 6** and **7**).

3.6. Histopathological analyses for adverse effects in vivo

To determine whether the DDS using Span 80 vesicles could prevent or reduce hazardous adverse effects due to the chemotherapeutic agents, the entire organs were histopathologically examined. Marked prevention of adverse effect was histopathologically

Treatment	Population of nonviable cells (%) (mean ± SD)
PV	1.6 ± 1.1
CV	1.4 ± 1.0
IFO	8.8 ± 1.9[a]
IV	10.2 ± 2.9[a]
IFO + CSB	16.5 ± 3.9[b]
IV + CSB	25.2 ± 4.2[b]
IFO + CV	32.8 ± 5.9[b]
IV + CV	97.1 ± 1.9[c]

[a]$P < 0.05$ versus PV and CV.
[b]$P < 0.05$ versus PV and CV.
[c]$P < 0.001$ versus PV and CV.

Table 2. Population of nonviable cells (M1) in flow cytometry.

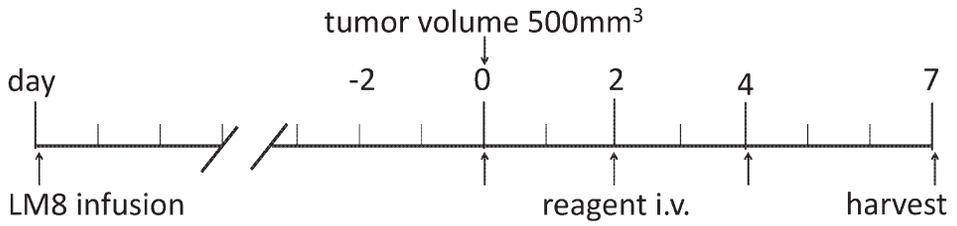

Figure 4. The in vivo therapeutic model. Administration of the antitumor agents was initiated when the tumor volume reached ~500 mm^3 (day 0), and continued on days 2 and 4. Then the mice were sacrificed and analyzed on day 7. [Reprinted with permission from Ref. [34]. Copyright (2014) Spandidos Publications].

observed in the kidney, liver, and testis. Significant tubular injury, which was recognized as a loss of brush border, as well as the glomerular damages such as the expansion of the mesangial matrix was manifested in the IFO-direct i.v. group in contrast to those in the IV and/or IV+CV groups (**Figure 8A** and **B**). Furthermore, in the liver, spotty or grouping necrosis as well as reduced glycogen storage in the hepatocytes was observed in the IFO-direct i.v. groups in contrast to those in the IV and IV + CV groups (**Figure 8C** and **D**). Moreover, the IV and IV + CV groups manifested no remarkable changes in spermatogenesis, while the IFO-direct i.v. group revealed marked suppression of spermatogenesis along with the necrosis of the germ cells (**Figure 8E** and **F**).

3.7. Fertility test

In order to elucidate whether the DDS with Span 80 nano-vesicles could be able to prevent the infertility, fertility tests were performed. Three male C3H/HeJ mice in each group that were administered IFO, IV, or IV + CV were cross-mated with 6-week-old female C3H/HeJ mice individually; then the fertility of each male was evaluated.

http://dx.doi.org/10.5772/intechopen.69155

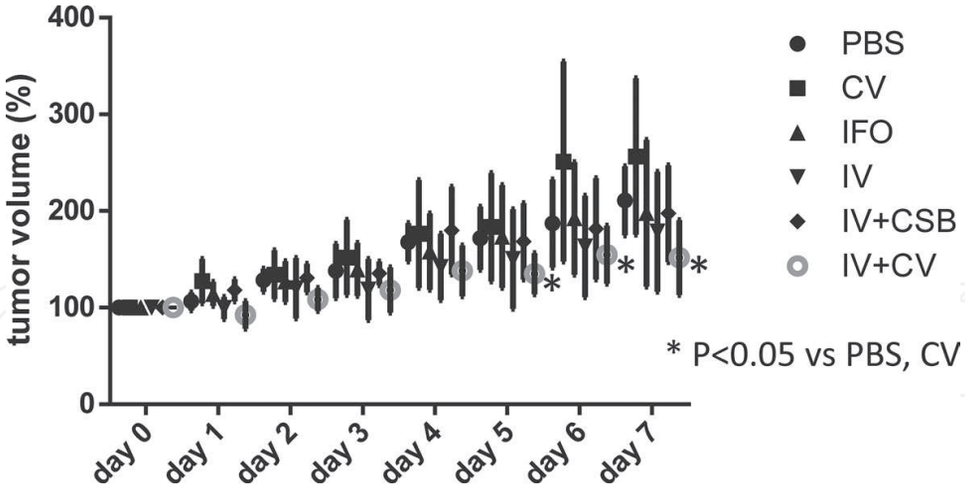

Figure 5. Trace of tumor volumes after antitumor agent administration. The symbols represent the mean value of each group, and the bars represent standard deviation. [Reprinted with permission from Ref. [34]. Copyright (2014) Spandidos Publications].

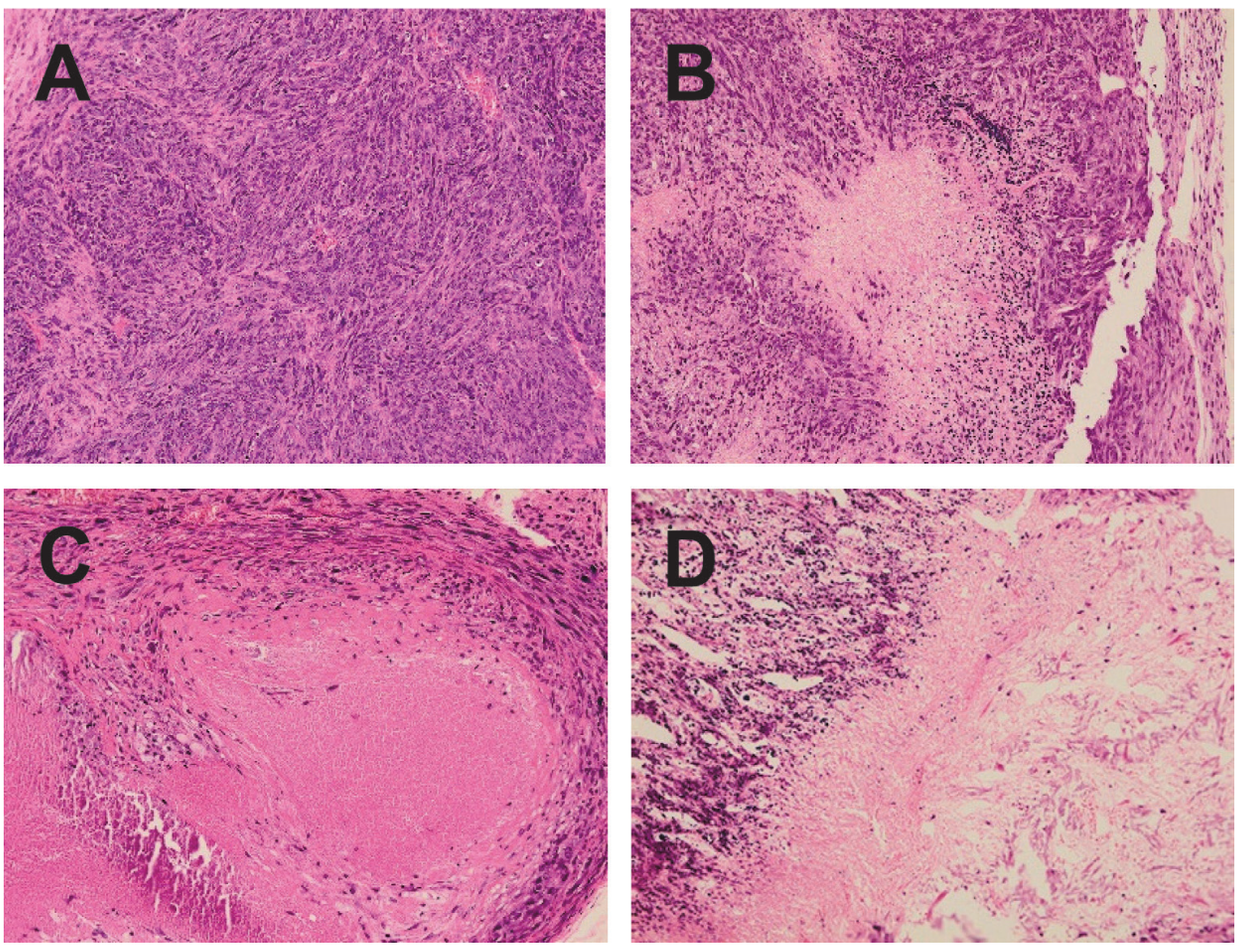

Figure 6. Representative photomicrographs of the tumors treated with (A) CV, (B) IFO, (C) IV, and (D) IV + CV. [Reprinted with permission from Ref. [34]. Copyright (2014) Spandidos Publications].

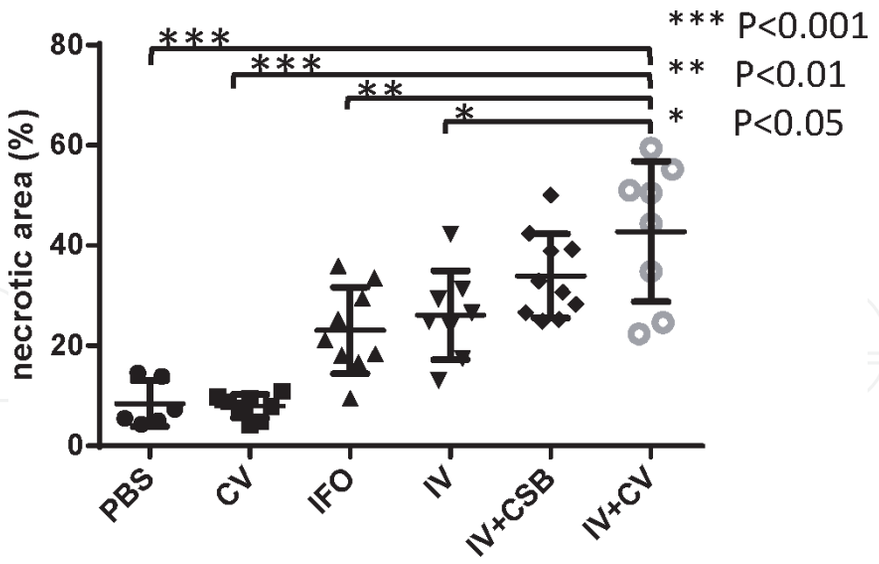

Figure 7. The nonviable tumor area (%) in each animal from each group. The center bars express mean value, as well as the upper and lower bars express standard deviation. [Reprinted with permission from Ref. [34]. Copyright (2014) Spandidos Publications].

The test revealed that the male mice after IV + CV administration had normal fertility, and there were no malformations in their progeny.

4. Discussion and conclusion

A promising suggestion from the therapeutic model of the DDS with Span 80 vesicles was conducted that this DDS could enhance the therapeutic effects of IFO and caffeine-potentiated IFO chemotherapy, over and above prevent the hazardous adverse effects induced by chemotherapy. In vitro studies revealed drastic cell death in a very early phase by IV + CV administration in contrast to the "mild" apoptotic cell death inference by the administration of IFO alone, IV alone, or combinations of IFO + CSB, IV + CSB, and IFO + CV. These findings suggested that the immediate delivery of therapeutic agents into the cytosol by IV + CV addition might induce extremely rapid apoptosis. Fusion of Span 80 vesicles and cell membrane could be implicated in this rapid response; nevertheless, the comprehensive mechanisms are still unknown.

Marked development of the DDS employing nano-vesicles has been reported along with the development of many types of phospholipids and/or detergents [6–8, 38]. The Span 80 nano-vesicle might be a promising material among them, based on its favorable physicochemical properties, including membrane fluidity and flexibility. With respect to membrane fluidity, Hayashi et.al. reported that Span 80 vesicles have markedly high fluidity with various cholesterol contents in comparison to conventional phospholipid liposomes, such as 1,2-dipalmitoyl-sn-glycero-3-phosphocholine and 1-palmitoyl-2-oleoyl-sn-glycero-3-phosphocholine liposomes. Not only the high fluidity, also Span 80 vesicles manifest much more flexibility in comparison to DPPC and POPC liposomes [26].

http://dx.doi.org/10.5772/intechopen.69155

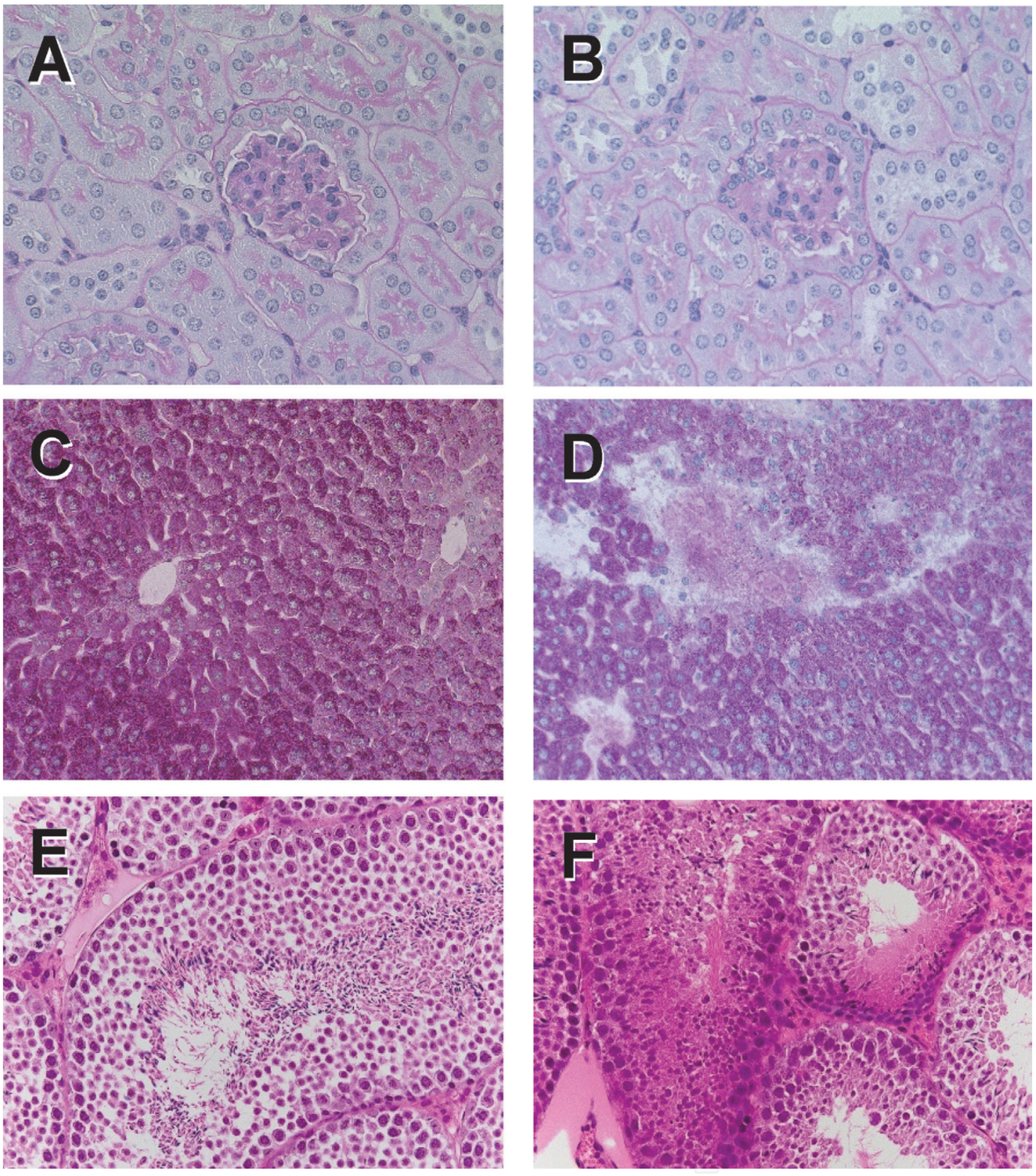

Figure 8. Representative histopathological characteristics of the renal tissue (A and B), liver (C and D), and testis (E and F), which were harvested from the animals with IV+CV (A, C, and E) and IFO i.v. (B, D, and F) administration.

Nonvesicular aggregates are observed often in the common liposome suspensions; on the other hand, Span 80 vesicle suspensions also could contain limited amount of nonvesicular aggregates such as tubulin structures. Recently, Kato et al. manifested that the Span 80 nanovesicle might be a kind of kinetically trapped aggregates and might not have thermodynamic equilibrium structures, like in most kinds of vesicles prepared from phosphatidylcholines (liposomes) [25].

The adverse effects induced by ifosfamide have been reported in kidney [35, 39–42], liver [43–45], gonadal cells [46–48], and bone marrow more frequently to other organs [49, 50]. In the therapeutic model of Span 80 DDS, the mice in the IFO-direct i.v. group also manifested moderate tubular injury as well as the glomerular damage in kidney, moreover, severe inhibition of spermatogenesis with gonadal cell necrosis. On the other hand, the novel DDS employing Span 80 nano-vesicles manifested marked prevention of the hazardous adverse effects in the kidney, liver, and testis. These favorable results could implicate the tumor selectivity of the Span80 vesicles, which might be at least partially resulting from the refraining from phagocytosis taken on the pegylation of the vesicles and also possibly on the lower permeability at the blood-testis barrier in comparison to the direct injection of low-molecular-weight molecules such as IFO [48, 51].

The results of our study indicated that higher vascular permeability and inclination to fuse with the instable cell membrane of the tumors based on high fluidity and flexibility as well as pegylation could result in the higher tumor selectivity of Span 80 vesicles [52]. Recently, a cell fusion model using Span 80 vesicles has been reported [27]. Furthermore, our results manifested that CV conducted markedly better enhancement of antitumor effects than that of the direct injection of CSB. This might be addressed by the pegylation-associated tumor selectivity as well as the inclination for cell fusion which might enable the immediate caffeine delivery into the cytoplasm. Moreover, the prevention of caffeine toxicity, which causes the withdrawal of numerous patients from caffeine-potentiated chemotherapy, could be prevented based on the selectivity of caffeine delivery by using Span 80 vesicles [5]. Currently, a DDS of doxorubicin containing liposomal nano-vesicles is applied in actual cancer therapy with marked efficacy [6–8, 53–55]. The next-generation liposomes with membrane-bound-targeting molecules have also been under development. An anticarcinoma application of Span 80 vesicles containing doxorubicin with or without membrane-bound-targeting molecule was recently reported [52]. As described above, Span 80 has favorable physicochemical properties; moreover, it also confirmed risk-free information because it has been already used as a stabilizer for injected drugs. Furthermore, the cost of Span 80 vesicles should be drastically cheaper than common liposomes. Therefore, the DDS with Span 80 nano-vesicles might be a promising next-generation DDS.

Recently, a novel treatment method for lymph node metastasis using a lymphatic drug delivery system with nano-/microbubbles has been advocated [56–58]. Those reports suggested that the lymphatic DDS might drastically improve the tissue selectivity and response rates to the metastatic tumors which had been limited in the hematogenous administration of drugs resulting in poor prognosis. Furthermore, those models could prevent the systemic toxic effects of the treatment; nevertheless, they employed highly toxic doxorubicin as the antitumor agent. The caffeine-potentiated chemotherapy employing the DDS with Span 80 vesicles might have excellent affinity to this lymphatic administration and more effective and less harmful treatment onto the tumor with lymph-nodal metastasis.

In conclusion, the DDS with Span 80 vesicles may enhance the antitumor effects of IFO and of caffeine-potentiated IFO chemotherapy against osteosarcoma. Moreover, the usage of this DDS may suppress the adverse effects, which were induced by the chemotherapy. Thus, this

DDS model has promising importance for clinical application in the therapy of metastatic osteosarcoma as well as the primary tumors.

Acknowledgements

We would like to thank Dr Keita Hayashi (Nara National College of Technology) and Dr Yosuke Omokawa (Nanocareer Inc. Ltd.) for their kind technical support, permission of documentation of their data, and useful advice. We are also deeply thankful to Professor Peter Walde (ETH, Zürich, Switzerland) for his helpful scientific discussion and advice. This study was supported by JSPS Kakenhi Grant Numbers 23592191, 25460496, and 16K08735.

Author details

Tatsuhiko Miyazaki[1]*, Hiroshi Nakata[2] and Keiichi Kato[3]

*Address all correspondence to: tats_m@gifu-u.ac.jp

1 Pathology Division, Gifu University Hospital, Gifu, Japan

2 Department of Orthopaedic Surgery, HITO Hospital, Shikokuchuo City, Japan

3 Ehime University Graduate School of Science and Engineering, Matsuyama, Japan

References

[1] Wu PK, Chen WM, Chen CF, Lee OK, Haung CK, Chen TH. Primary osteogenic sarcoma with pulmonary metastasis: Clinical results and prognostic factors in 91 patients. Japanese Journal of Clinical Oncology. 2009;**39**(8):514–522. DOI: 10.1093/jjco/hyp057

[2] Clark JC, Dass CR, Choong PF. A review of clinical and molecular prognostic factors in osteosarcoma. Journal of Cancer Research and Clinical Oncology. 2008;**134**(3):281–297. DOI: 10.1007/s00432-007-0330-x

[3] Kimura H, Tsuchiya H, Shirai T, Nishida H, Hayashi K, Takeuchi A, Ohnari I, Tomita K. Caffeine-potentiated chemotherapy for metastatic osteosarcoma. Journal of Orthopaedic Science. 2009;**14**(5):556–565. DOI: 10.1007/s00776-009-1372-5

[4] Tsuchiya H, Tomita K, Mori Y, Asada N, Morinaga T, Kitano S, Yamamoto N. Caffeine-assisted chemotherapy and minimized tumor excision for nonmetastatic osteosarcoma. Anticancer Research. 1998;**18**(1B):657–666

[5] Hayashi K, Tsuchiya H, Yamamoto N, Shirai T, Yamauchi K, Takeuchi A, Kawahara M, Miyamoto K, Tomita K. Impact of serum caffeine monitoring on adverse effects and

chemotherapeutic responses to caffeine-potentiated chemotherapy for osteosarcoma. Journal of Orthopaedic Science. 2009;**14**(3):253–258. DOI: 10.1007/s00776-009-1336-9

[6] Yang C, Fu ZX. Liposomal delivery and polyethylene glycol-liposomal oxaliplatin for the treatment of colorectal cancer (review). Biomedical Reports. 2014;**2**(3):335–339. DOI: 10.3892/br.2014.249

[7] Brochu H, Polidori A, Pucci B, Vermette P. Drug delivery systems using immobilized intact liposomes: A comparative and critical review. Current Drug Delivery. 2004;**1**(3): 299–312

[8] Sultana S, Khan MR, Kumar M, Kumar S, Ali M. Nanoparticles-mediated drug delivery approaches for cancer targeting: A review. Journal of Drug Targeting. 2013;**21**(2):107–125. DOI: 10.3109/1061186X.2012.712130

[9] Bangham AD, Standish MM, Watkins JC. Diffusion of univalent ions across the lamellae of swollen phospholipids. Journal of Molecular Biology. 1965;**13**(1):238–252

[10] Vanlerberghe G. Niosomes and other non-phospholipid vesicular systems. In: Uchegbu IF, editor. Synthetic Surfactant Vesicles. Amsterdam: Harwood Academic Publishers; 2000. pp. 3–7

[11] Fendler JH. Membrane Mimetic Chemistry. New York, NY: Wiley and Sons; 1982

[12] Lasic DD. Liposomes. Physics to Applications. Amsterdam: Elsevier; 1993

[13] Lasic DD. Novel applications of liposomes. Trends in Biotechnology. 1998;**16**(7): 307–321

[14] Storm G, ten Kate MT, Working PK, Bakker-Woudenberg IA. Doxorubicin entrapped in sterically stabilized liposomes: Effects on bacterial blood clearance capacity of the mononuclear phagocyte system. Clinical Cancer Research: An Official Journal of the American Association for Cancer Research. 1998;**4**(1):111–115

[15] Torchilin VP. Recent advances with liposomes as pharmaceutical carriers. Nature Reviews Drug Discovery. 2005;**4**(2):145–160. DOI: 10.1038/nrd1632

[16] Gibbs BF, Kermasha S, Alli I, Mulligan CN. Encapsulation in the food industry: A review. International Journal of Food Science Nutrition. 1999;**50**(3):213–224

[17] Taylor TM, Davidson PM, Bruce BD, Weiss J. Liposomal nanocapsules in food science and agriculture. Critical Reviews in Food Science and Nutrition. 2005;**45**(7–8):587–605. DOI: 10.1080/10408390591001135

[18] Edwards KA, Baeumner AJ. Liposomes in analyses. Talanta. 2006;**68**(5):1421–1431

[19] Monnard PA, Deamer DW. Membrane self-assembly processes: Steps toward the first cellular life. The Anatomical Record. 2002;**268**(3):196–207. DOI: 10.1002/ar.10154

[20] Luisi PL, Ferri F, Stano P. Approaches to semi-synthetic minimal cells: a review. Naturwissenschaften. 2006;**93**(1):1–13. DOI: 10.1007/s00114-005-0056-z

[21] Uchegbu IF, Vyas SP. Non-ionic surfactant based vesicles (niosomes) in drug delivery. International Journal of Pharmaceutics. 1998;**172**(1–2):33–70. http://dx.doi.org/10.1016/S0378-5173(98)00169-0

[22] Uchegbu IF, Florence AT. Non-ionic surfactant vesicles (niosomes): Physical and pharmaceutical chemistry. Advances in Colloid and Interface Science. 1995;**581**(1):1–55

[23] Wang ZF, M. Analysis of sorbitan ester surfactants. 2. Capillary supercritical-fluid chromatography. High Resolution Chromatography. 1994;**17**:85–90

[24] Cottrell, T. van Peij, J. Sorbitan esters and polysorbates. In: Whitehurst RJ, editor. Emulsifiers in Food Technology. Oxford: Blackwell Publishing Ltd.; 2004. pp. 162–185

[25] Kato K, Walde P, Koine N, Ichikawa S, Ishikawa T, Nagahama R, Ishihara T, Tsujii T, Shudou M, Omokawa Y, Kuroiwa T. Temperature-sensitive nonionic vesicles prepared from Span 80 (sorbitan monooleate). Langmuir: The ACS Journal of Surfaces and Colloids. 2008;**24**(19):10762–10770. DOI: 10.1021/la801581f

[26] Hayashi K, Shimanouchi T, Kato K, Miyazaki T, Nakamura A, Umakoshi H. Span 80 vesicles have a more fluid, flexible and "wet" surface than phospholipid liposomes. Colloids and Surfaces B: Biointerfaces. 2011;**87**(1):28–35. DOI: 10.1016/j.colsurfb.2011.04.029

[27] Hayashi K, Tatsui T, Shimanouchi T, Umakoshi H. Membrane interaction between Span 80 vesicle and phospholipid vesicle (liposome): Span 80 vesicle can perturb and hemifuse with liposomal membrane. Colloids and Surfaces B: Biointerfaces. 2013;**106**:258–264. DOI: 10.1016/j.colsurfb.2012.12.022

[28] Omokawa Y, Miyazaki T, Walde P, Akiyama K, Sugahara T, Masuda S, Inada A, Ohnishi Y, Saeki T, Kato K. In vitro and in vivo anti-tumor effects of novel Span 80 vesicles containing immobilized Eucheuma serra agglutinin. International Journal of Pharmaceuticals. 2010;**389**(1–2):157–167. DOI: 10.1016/j.ijpharm.2010.01.033

[29] Brandner JD. The composition of NF-defined emulsifiers: Sorbitan monolaurate, monopalmitate, monostearate, monooleate, polysorbate 20, polysorbate 40, polysorbate 60, and polysorbate 80. Drug Development and Industrial Pharmacy. 1998;**24**(11):1049–1054. DOI: 10.3109/03639049809089948

[30] Lu DR, Rhodes D.G. Mixed compositions films of Spans and Tween-80 at the air-water interface. Langmuir: The ACS Journal of Surfaces and Colloids. 2000;**16**:8107–8112

[31] Yoshioka, T. Stermberg, B. Florence, A.T. Preparation and properties of vesicles (niosomes) of sorbitan monoesters (Span 20, 40, 60, and 80) and a sorbitan triester (Span 85). International Journal of Pharmaceuticals. 1994;**105**:1–6

[32] Kono K, Takagishi T. Temperature-sensitive liposomes. Methods in Enzymology. 2004; **387**:73–82. DOI: 10.1016/S0076-6879(04)87005-8

[33] Needham D, Dewhirst MW. The development and testing of a new temperature-sensitive drug delivery system for the treatment of solid tumors. Advanced Drug Delivery Reviews. 2001;**53**(3):285–305

[34] Nakata H, Miyazaki T, Iwasaki T, Nakamura A, Kidani T, Sakayama K, Masumoto J, Miura H. Development of tumor-specific caffeine-potentiated chemotherapy using a novel drug delivery system with Span 80 nano-vesicles. Oncological Reports. 2015;**33**(4):1593–1598. DOI: 10.3892/or.2015.3761

[35] Oberlin O, Fawaz O, Rey A, Niaudet P, Ridola V, Orbach D, Bergeron C, Defachelles AS, Gentet JC, Schmitt C, Rubie H, Munzer M, Plantaz D, Deville A, Minard V, Corradini N, Leverger G, de Vathaire F. Long-term evaluation of ifosfamide-related nephrotoxicity in children. Journal of Clinical Oncology. 2009;**27**(32):5350–5355. DOI: 10.1200/jco.2008.17.5257

[36] Hotz MA, Gong J, Traganos F, Darzynkiewicz Z. Flow cytometric detection of apoptosis: Comparison of the assays of in situ DNA degradation and chromatin changes. Cytometry. 1994;**15**(3):237–244. DOI: 10.1002/cyto.990150309

[37] Asai T, Ueda T, Itoh K, Yoshioka K, Aoki Y, Mori S, Yoshikawa H. Establishment and characterization of a murine osteosarcoma cell line (LM8) with high metastatic potential to the lung. International Journal of Cancer. 1998;**76**(3):418–422

[38] Elbayoumi TA, Torchilin VP. Enhanced cytotoxicity of monoclonal anticancer antibody 2C5-modified doxorubicin-loaded PEGylated liposomes against various tumor cell lines. European Journal of Pharmaceutical Science. 2007;**32**(3):159–168. DOI: 10.1016/j.ejps.2007.05.113

[39] Skinner R, Cotterill SJ, Stevens MC. Risk factors for nephrotoxicity after ifosfamide treatment in children: A UKCCSG Late Effects Group study. United Kingdom Children's Cancer Study Group. British Journal of Cancer. 2000;**82**(10):1636–1645. DOI: 10.1054/bjoc.2000.1214

[40] Patterson WP, Khojasteh A. Ifosfamide-induced renal tubular defects. Cancer. 1989;**63**(4):649–651

[41] Skinner R, Pearson AD, Coulthard MG, Skillen AW, Hodson AW, Goldfinch ME, Gibb I, Craft AW. Assessment of chemotherapy-associated nephrotoxicity in children with cancer. Cancer Chemotherapy and Pharmacology. 1991;**28**(2):81–92

[42] McCune JS, Friedman DL, Schuetze S, Blough D, Magbulos M, Hawkins DS. Influence of age upon ifosfamide-induced nephrotoxicity. Pediatric Blood Cancer. 2004;**42**(5):427–432. DOI: 10.1002/pbc.20011

[43] Wagner T. Ifosfamide clinical pharmacokinetics. Clinical Pharmacokinetics. 1994;**26**(6):439–456. DOI: 10.2165/00003088-199426060-00003

[44] Howell JE, Szabatura AH, Hatfield Seung A, Nesbit SA. Characterization of the occurrence of ifosfamide-induced neurotoxicity with concomitant aprepitant. Journal of Oncology Pharmacy Practice. 2008;**14**(3):157–162. DOI: 10.1177/1078155208093930

[45] Cheung MC, Jones RL, Judson I. Acute liver toxicity with ifosfamide in the treatment of sarcoma: A case report. Journal of Medical Case Reports. 2011;**5**:180. DOI: 10.1186/1752-1947-5-180

[46] Yonemoto T, Ishii T, Takeuchi Y, Hagiwara Y, Iwata S, Tatezaki S. Recently intensified chemotherapy for high-grade osteosarcoma may affect fertility in long-term male survivors. Anticancer Research. 2009;**29**(2):763–767

[47] Ridola V, Fawaz O, Aubier F, Bergeron C, de Vathaire F, Pichon F, Orbach D, Gentet JC, Schmitt C, Dufour C, Oberlin O. Testicular function of survivors of childhood cancer: A comparative study between ifosfamide- and cyclophosphamide-based regimens. European Journal of Cancer. 2009;**45**(5):814–818. DOI: 10.1016/j.ejca.2009.01.002

[48] Longhi A, Macchiagodena M, Vitali G, Bacci G. Fertility in male patients treated with neoadjuvant chemotherapy for osteosarcoma. Journal of Pediatric Hematology/Oncology. 2003;**25**(4):292–296

[49] Thomson B, Hawkins D, Felgenhauer J, Radich J. RT-PCR evaluation of peripheral blood, bone marrow and peripheral blood stem cells in children and adolescents undergoing VACIME chemotherapy for Ewing's sarcoma and alveolar rhabdomyosarcoma. Bone Marrow Transplantation. 1999;**24**(5):527–533. DOI: 10.1038/sj.bmt.1701939

[50] Lotz JP, Andre T, Donsimoni R, Firmin C, Bouleuc C, Bonnak H, Merad Z, Esteso A, Gerota J, Izrael V. High dose chemotherapy with ifosfamide, carboplatin, and etoposide combined with autologous bone marrow transplantation for the treatment of poor-prognosis germ cell tumors and metastatic trophoblastic disease in adults. Cancer. 1995;**75**(3):874–885

[51] Williams D, Crofton PM, Levitt G. Does ifosfamide affect gonadal function? Pediatric Blood Cancer. 2008;**50**(2):347–351. DOI: 10.1002/pbc.21323

[52] Hayashi K, Tatsui T, Shimanouchi T, Umakoshi H. Enhanced cytotoxicity for colon 26 cells using doxorubicin-loaded sorbitan monooleate (Span 80) vesicles. International Journal of Biological Science. 2013;**9**(2):142–148. DOI: 10.7150/ijbs.5453

[53] Iwamoto T. Clinical application of drug delivery systems in cancer chemotherapy: Review of the efficacy and side effects of approved drugs. Biological & Pharmaceutical Bulletin. 2013;**36**(5):715–718

[54] Eckes J, Schmah O, Siebers JW, Groh U, Zschiedrich S, Rautenberg B, Hasenburg A, Jansen M, Hug MJ, Winkler K, Putz G. Kinetic targeting of pegylated liposomal doxorubicin: A new approach to reduce toxicity during chemotherapy (CARL-trial). BMC Cancer. 2011;**11**:337. DOI: 10.1186/1471-2407-11-337

[55] Maeng JH, Lee DH, Jung KH, Bae YH, Park IS, Jeong S, Jeon YS, Shim CK, Kim W, Kim J, Lee J, Lee YM, Kim JH, Kim WH, Hong SS. Multifunctional doxorubicin loaded superparamagnetic iron oxide nanoparticles for chemotherapy and magnetic resonance imaging in liver cancer. Biomaterials. 2010;**31**(18):4995–5006. DOI: 10.1016/j.biomaterials.2010.02.068

[56] Kato S, Mori S, Kodama T. A novel treatment method for lymph node metastasis using a lymphatic drug delivery system with nano/microbubbles and ultrasound. Journal of Cancer. 2015;**6**(12):1282–1294. DOI: 10.7150/jca.13028

[57] Kato S, Shirai Y, Kanzaki H, Sakamoto M, Mori S, Kodama T. Delivery of molecules to the lymph node via lymphatic vessels using ultrasound and nano/microbubbles. Ultrasound in Medicine & Biology. 2015;**41**(5):1411–1421. DOI: 10.1016/j.ultrasmedbio.2014.12.014

[58] Sato T, Mori S, Arai Y, Kodama T. The combination of intralymphatic chemotherapy with ultrasound and nano-/microbubbles is efficient in the treatment of experimental tumors in mouse lymph nodes. Ultrasound in Medicine & Biology. 2014;**40**(6):1237–1249. DOI: 10.1016/j.ultrasmedbio.2013.12.012

IntechOpen